Effect of halogenated compounds on the photophysics of C_{70} and a monoadduct of C_{70}: Some implications on optical limiting behaviour

Sarah Foley [a], Mário N. Berberan-Santos [a,*], Aleksandre Fedorov [a],
René V. Bensasson [b], Sydney Leach [c], Bárbara Gigante [d]

[a] *Centro de Química-Física Molecular, Instituto Superior Técnico, 1049-001 Lisbon, Portugal*
[b] *Laboratoire de Biophysique, Muséum National d'Histoire Naturelle, 43 rue Cuvier, 75231 Paris Cedex, France*
[c] *DAMAP, CNRS UMR 8588, Observatoire de Paris-Meudon, 92195 Meudon, France*
[d] *INETI-IBQTA, Departamento de Tecnologia e Indústrias Químicas, Estrada do Paço do Lumiar, 1649-038 Lisbon, Portugal*

Received 18 September 2000

Abstract

The fluorescence spectra, quantum yields and lifetimes of C_{70} and a pseudo-dihydro derivative ($C_{70}R$) have been measured in a wide range of solvents at room temperature. This information is important for the development of reverse saturable absorbers. Phosphorescence spectra and phosphorescence lifetimes were also measured at low temperature. The fluorescence is subject to quenching by halogenated compounds. The efficiency of quenching follows the order $I > Br \gg Cl$. The nature of the quenching is shown to vary, with chlorinated compounds exhibiting static quenching of fullerene fluorescence, owing to nonfluorescent complex formation, whilst those compounds containing bromine and iodine exhibit dynamic quenching due to the external heavy-atom effect, that increases the intersystem crossing rate constant in the fluorophore–perturber complex. This constant is evaluated by an original method from the bimolecular quenching rate constants. The phosphorescence quantum yield of both fullerenes at 77 K slightly increases in the presence of iodobenzene, in spite of a strong decrease in phosphorescence lifetime. The marked increase of the intersystem crossing rate constant in concentrated solutions owing to the external heavy-atom effect is of interest for the application of fullerenes as fast-responding optical limiters (reverse saturable absorbers) of intense laser pulses, even in cases where the triplet quantum yield is of the order of unity. © 2001 Elsevier Science B.V. All rights reserved.

1. Introduction

The quenching of fluorescence by heavy atoms (i.e., atoms of large atomic number), a phenomenon identified as physical quenching by Francis Perrin in 1926 [1–3], has been the subject of a number of studies [4–19]. Heavy-atom quenching of fluorescence may occur in two different ways. Firstly, the heavy atom can be part of the chromophore under study; this is referred to as the internal heavy-atom effect [4,6]. In the external heavy-atom effect [5,6], the quencher is external to the chromophore, either intramolecularly (quenching moiety [11,14], as in naphthylalkyl iodides [11])

* Corresponding author. Tel.: +351-21-841-9219; fax: +351-21-846-4455.
E-mail address: berberan@ist.utl.pt (M.N. Berberan-Santos).

or intermolecularly, as the quencher (e.g. I^-, Xe) or part of the quencher (e.g. CH_3I, $Hg(CH_3)_2$). The external process requires close contact between perturber and fluorophore, usually in the form of a statistical (contact) charge-transfer complex (exciplex with binding energy smaller than kT). In fluid media, this complex is short-lived, as it is both brought about and broken apart by the incessant diffusive motion of quencher and fluorophore. In rigid media, e.g. low temperature organic glasses, diffusion is prevented and the quenching is static: the perturber is effective only in statistical pairs, trios, etc. that were trapped upon cooling.

McClure's [4] theoretical and experimental results, as well as the experiments by Kasha [5], conclusively showed that the spin–orbit coupling strengthening by large atomic numbers, previously observed in atomic spectra (e.g. Hg), was also possible in molecules. The decrease of fluorescence quantum yield (radiative transition $S_1 \rightarrow S_0$) is thus in most cases explained by an increase in the probability of the competing $S_1 \rightarrow T_n$ radiationless transition of the fluorophore. In some exceptional cases however, the incorporation of one or more heavy atoms in the molecule (internal effect) significantly shifts the singlet and triplet energy levels with respect to those of the unperturbed chromophore [20], modifying its photophysics in a manner unrelated to spin–orbit coupling strength variation.

The internal heavy-atom effect, resulting from the substitution of one or more light atoms (usually hydrogens) by heavy atoms (usually bromines or iodines) on a given chromophore, is gauged by the concomitant increase of the $S_1 \rightarrow T_n$ intersystem crossing rate constant. In the case of the external heavy atom effect in fluid solution, simple Stern–Volmer kinetics is observed, and the effect is usually gauged by the magnitude of the bimolecular quenching rate constant [7,9,10,13,20,21]. It was recently pointed out that it is also possible to obtain from the experimental results the unimolecular $S_1 \rightarrow T_n$ intersystem crossing rate constant of the perturbed fluorophore [22]. It is this constant that can be directly compared with that of the unperturbed fluorophore.

In fluid solution, two distinct quenching processes of singlet excited molecules M* by molecules Q, both implying molecular contact, are known [20,21]: (a) Static quenching, which involves the formation of a stable nonfluorescent complex. The emission lifetime of M* remains constant but the luminescence intensity decreases with [Q], the concentration of Q. (b) Dynamic quenching, where the molecules M* and Q come into contact through their random, diffusional motion. In this case, both the fluorescence quantum yield and the lifetime of M* decrease with [Q]. This is usually the situation for external heavy atom quenching. Also for contact quenching, a further static process is possible [22] in rigid solution: for high concentrations of quencher, a significant fraction of statistical contact pairs, trios, etc. are trapped in the rigid matrix, and the fluorescence intensity is partially quenched, while the fluorescence decay becomes nonexponential [22].

The photophysics of C_{70} and monoderivatives is dominated by a very efficient intersystem crossing (quantum yield of triplet formation close to one [23]). It is therefore of interest to investigate if the intersystem crossing rate can be enhanced by the action of external perturbers, namely by the external heavy atom effect. This should be relevant to the use of fullerenes as optical limiters by reverse saturable absorption (RSA). There is presently great interest in materials with these nonlinear transmission properties, and the study of RSA by fullerenes is actively pursued [24–26].

In this paper, the fluorescence quantum yields and singlet state lifetimes of both C_{70} and $C_{70}R$ (a pseudo-dihydro derivative of C_{70}) have been measured in both hydrocarbon solvents and halogenated solvents at room temperature, investigating the heavy atom effect on fluorescence quenching and the relative importance of the static and dynamic quenching mechanisms. This information as well as the relative phosphorescence quantum yield of the two fullerenes at 77 K in various solvents enabled us to determine the effect of heavy atoms on the nonradiative intersystem crossing rate as well as the radiative constant for phosphorescence.

2. Experimental

2.1. Materials

$C_{70}(>99\%)$ was obtained from Stefan Kaesdorf (Munich, Germany) and was used as received. The C_{70} monoadduct ($C_{70}R$) shown in Fig. 1, structurally a pseudo-dihydrofullerene, was synthesized as described previously [23,27].

All solvents used were of spectroscopic grade. For phosphorescence measurements two solvent mixtures were used: (a) methylcyclohexane–toluene (7:2, v/v), denoted MT and, (b) MT + 10% v/v iodobenzene, denoted MTI. Both give good clear glasses at 77 K.

2.2. Instrumentation and methods

Fluorescence spectra were obtained with a SPEX Fluorolog F112A fluorimeter. Fluorescence quantum yields (ϕ_f) for C_{70} and $C_{70}R$ at room temperature were determined using solutions of C_{70} in toluene as the reference, for which [28] $\phi_f = 5.7 \times 10^{-4}$. For this purpose, the usual procedures were followed; namely, optical densities were matched, and refractive indexes corrections applied.

Singlet state lifetimes were determined using the single photon timing method as described previously [29]. Phosphorescence spectra at 77 K were obtained in the above mentioned fluorimeter using a specially adapted Aminco rotatin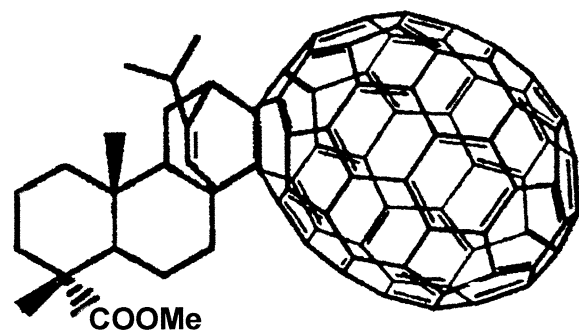g can phosphorescence head. The excitation wavelength was always 460 nm. Phosphorescence lifetimes at 77 K were measured by the modulation method, using a CW argon ion laser (514 nm) whose beam was passed through a mechanical chopper to produce equally spaced (typical period: 200 ms) 80 mJ square pulses with a duration of 5 ms. The emitted luminescence was passed through a RG695 filter before detection by a fast photodiode coupled to an oscilloscope.

3. Results and discussion

3.1. Steady state fluorescence

Figs. 2 and 3 show the normalized fluorescence spectra of C_{70} and $C_{70}R$, respectively, in a range of solvents at room temperature. As can be seen, the fluorescence maximum is red shifted on moving down the halogen series in both cases. A change in relative vibronic intensities in C_{70} when going from methylcyclohexane to bromobenzene is also evident: the first maximum, located at 652 nm in cyclohexane, red shifts and is intensified with respect to the second maximum, located at 696 nm in cyclohexane. This is similar to the observation made by Sun et al. [30] in hexane–tetrahydrofuran (THF) mixtures when increasing the THF fraction. The at the time puzzling "reverse Ham behaviour" can now be analysed in the light of recent
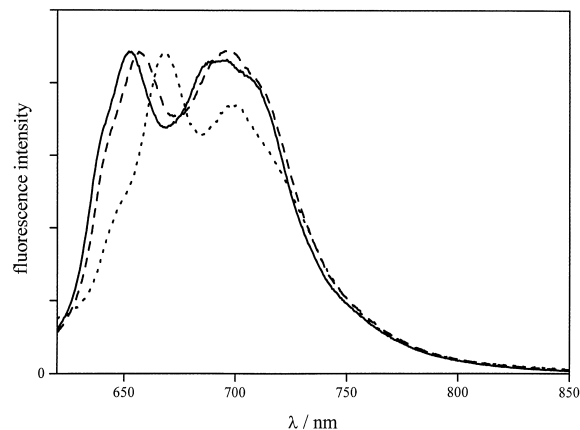
Fig. 1. Structure of the α-monoadduct of C_{70}, of the pseudo-dihydroderivative type (only one of the two isomers is shown).

Fig. 2. Normalised fluorescence spectra of C_{70} in methylcyclohexane (—), CCl_4 (- - -) and bromobenzene (· · ·).
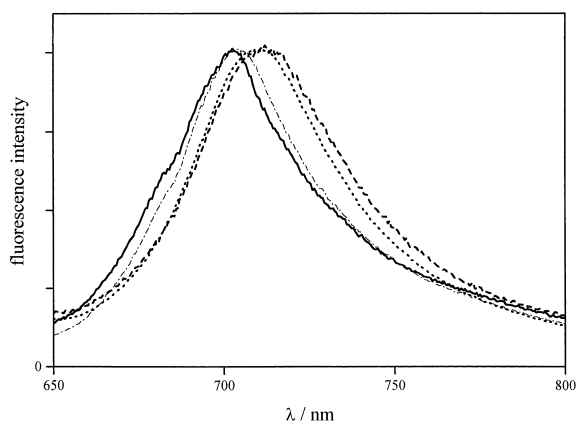
Fig. 3. Normalised fluorescence spectra of $C_{70}R$ in methylcyclohexane (—), CCl_4 (·--·), bromobenzene (···) and methyl iodide (- - -).

experimental and theoretical studies [18,31–34]. These showed that the first peak, located at 652 nm in methylcyclohexane, is associated with the weakly allowed $S_2 \rightarrow S_0$ transition, while the shoulder, located at ≈ 660 nm in methylcyclohexane (not apparent in Fig. 2 owing to the wide emission band passes used), corresponds to the nearly forbidden $S_1 \rightarrow S_0$ transition. An increased interaction with the solvent has thus the expected effect of preferential enhancement of the 660 nm transition, along with some red shift (668 nm in bromobenzene).

As can be seen in Fig. 3, the emission of $C_{70}R$ is structureless, and its maximum intensity occurs at

702 nm in methylcyclohexane, 704 nm in CCl_4, 709 nm in bromobenzene and 712 nm in CH_3I.

3.2. Fluorescence quantum yields

As summarized in Tables 1 and 2, ϕ_f values ranged from 6×10^{-4} to 2×10^{-4} for C_{70} in methylcyclohexane and dibromomethane solvents respectively, and from 7×10^{-4} to 5×10^{-5} for $C_{70}R$ in dodecane and methyl iodide solvents respectively. The ϕ_f values are very similar for each fullerene in similar solvents.

3.3. Fluorescence lifetimes

The singlet state lifetimes of both C_{70} and $C_{70}R$ are collected together in Tables 1 and 2. Lifetimes for C_{70} vary from 0.65 ns to 20 ps in methylcyclohexane and methyl iodide solvents respectively. For $C_{70}R$, lifetimes vary from 1.1 ns to 70 ps in dodecane and methyl iodide solvents respectively. The lifetimes observed in hydrocarbon and chlorinated solvents have nearly constant values. For bromo and iodo substituted solvents there is a marked reduction in fluorescence lifetimes.

3.4. Fluorescence quenching

As is evident from Tables 1 and 2 quenching of fullerene fluorescence occurs in all halogenated solvents as shown by a reduction in fluorescence quantum yields.

Table 1
Fluorescence quantum yields and average singlet state lifetimes for C_{70} in various solvents at room temperature

Solvent	$\phi_f/10^{-4}$	τ (ns)	Quenching process
Methylcyclohexane	6.0	0.65	–
Toluene	5.7[a]	0.65	–
Dichloromethane	4.6	0.63	Static (nonfluorescent complex)
Chloroform	4.5	0.60	″
Carbon tetrachloride	5.1	0.60	″
Chlorobenzene	5.4	0.60	″
Dibromomethane	2.0	0.25	Dynamic
Bromoform	2.3	0.25	″
Bromobenzene	2.5	0.28	″
Methyl iodide	–	0.02	Dynamic
Ethyl iodide	–	0.11	″
Iodobenzene	–	0.13	″

[a] Reference value, taken from Ref. [28].

Table 2
Fluorescence quantum yields and average singlet state lifetimes for $C_{70}R$ in various solvents at room temperature

Solvent	$\phi_f/10^{-4}$	τ (ns)	Quenching process
Dodecane	7.2	1.1	–
Carbon disulphide	7.2	1.0	–
Methylcyclohexane	6.6	1.1	–
Toluene	6.2	1.1	–
DMF	5.8	1.1	–
Dichloromethane	4.1	1.0	Static (nonfluorescent complex)
Chloroform	4.1	1.0	"
Carbon tetrachloride	4.4	1.1	"
Chlorobenzene	5.2	1.1	"
Dibromomethane	2.8	0.4	Dynamic
Bromoform	3.4	0.4	"
Bromobenzene	2.6	0.4	"
Methyl iodide	0.5	0.07	Dynamic
Ethyl iodide	1.2	0.09	"
Iodobenzene	1.4	0.12	"

The quenching of fluorescence of the fullerenes is shown in this section to be both static, in chlorinated solvents, and dynamic in bromo and iodo substituted solvents, as indicated in Tables 1 and 2. Both cases will be discussed in turn.

3.4.1. Static quenching

With reference to Tables 1 and 2 it can be seen that the fluorescence quantum yields in chlorinated solvents are reduced with respect to those obtained for hydrocarbon solvents such as toluene and methylcyclohexane. However, the singlet state lifetimes remain almost constant at 0.60–0.65 ns and 1.0–1.1 ns for C_{70} and $C_{70}R$ respectively. Such results are indicative of predominant static quenching, i.e., the transition probability of the emitting fluorophores remains practically unchanged.

The fluorescence spectrum of $C_{70}R$ in methylcyclohexane, containing chloroform as the quencher, maintains its shape but shows a decrease in intensity as a consequence of the above-mentioned static quenching process. Using the Stern–Volmer equation for static quenching by nonfluorescent complex formation,

$$\frac{I_f^0}{I_f} = 1 + K_{SV}[Q], \tag{1}$$

by which K_{SV} is equal to the association constant of the nonfluorescent complex, K_e, it is possible to determine this association constant from a plot of I_f^0/I_f versus the concentration of the quencher. This plot is shown in Fig. 4 for $C_{70}R$ in methylcyclohexane–chloroform mixtures. The determined Stern–Volmer constants are 3.0×10^{-2} dm^3 mol^{-1} and 5.3×10^{-2} dm^3 mol^{-1} for C_{70} and $C_{70}R$, respectively. These equilibrium association constants are very small and they show a negligible affinity between the fullerenes and the chlorinated solvents, which appear to form statistical contact complexes only. The measured values of the equilibrium
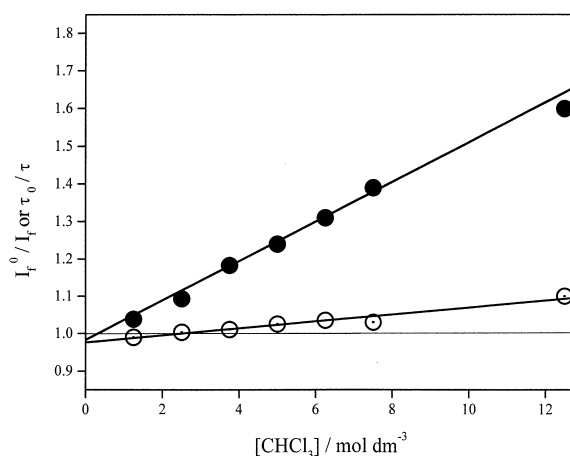

Fig. 4. Stern–Volmer plots for the quenching of $C_{70}R$ fluorescence in methylcyclohexane by CHCl$_3$: ($\odot$) lifetimes ratio (τ_0/τ) and ($\bullet$) intensities ratio (I_f^0/I_f).

association constants with chlorinated compounds are similar to those previously found for some aromatic hydrocarbons [35].

From K_e and using Eq. (2) below it is possible to estimate the fraction of fluorophore present as the nonfluorescent weak complex:

$$\alpha = \frac{K_e[Q]}{1 + K_e[Q]}. \tag{2}$$

The associated fractions in pure chloroform ([Q] = 12.5 mol dm^{-3}) determined for C_{70} and $C_{70}R$ are 0.3 and 0.4 respectively. Such values explain the reduction observed in the fluorescence quantum yields obtained in chlorinated solvents. Also evident from Fig. 4 is that the singlet state lifetimes for $C_{70}R$ remain almost constant irrespective of the concentration of chloroform present in the solution (results are similar for C_{70}, but data is not shown).

One of the main assumptions behind Stern–Volmer kinetics is the invariance of the radiative rate constant with quencher concentration. This is reasonable if the quencher solutions are relatively dilute. However, when the quenching study covers the entire composition range, from the pure solvent to the pure (liquid) quencher, the question arises as to the validity of such an assumption. Indeed, an apparent quenching could in our case be solely due to the decrease of the radiative rate constant. The lifetime would remain constant, because in the studied compounds it is dominated by the nonradiative rate constant, but the fluorescence quantum yield would decrease. However, if this were the case, the absorption spectrum would change, with a decrease of the absorption coefficients (at least) near the absorption onset, as a result of an increase of the quencher concentration. In separate experiments, the absorption (and excitation) spectra in pure hydrocarbon and in pure chlorinated solvent were shown to be practically identical. The alternative explanation can thus be ruled out. Furthermore, the usual effect of increased solvent polarity and polarizability on a weakly allowed transition, intensification, can lead to an increase of the radiative constant, owing to its proportionality to the oscillator strength of the first band, but not to the opposite effect. Our

spectral study shows that in chloroform this effect is also minor, if any. This may be explained by the fact that most vibronic transitions present in the emission spectrum are much less sensitive to the solvent perturbation than the 0–0 one.

3.4.2. Dynamic quenching

The addition of bromo and iodo substituted solvents to the fullerene solutions in methylcyclohexane also results in the quenching of fluorescence. In these cases the quenching is overwhelming dynamic, as noted by a similar reduction in fluorescence quantum yields and singlet state lifetimes.

For both C_{70} and $C_{70}R$, bromobenzene was used as the quencher, whilst methyl iodide was also used to quench the fluorescence of $C_{70}R$.

Quenching of the fluorescence of both C_{70} and $C_{70}R$ is determined with respect to the change in fluorescence intensity and also a reduction in singlet state lifetimes with increasing concentration of bromobenzene. Analysis is again made using the Stern–Volmer equation whereby $k_q\tau_0$ is substituted for K_{SV}, and

$$\frac{I_f^0}{I_f} = 1 + k_q\tau_0[Q]. \tag{3}$$

As before, a plot of I_f^0/I_f versus [Q] results in a straight line whose slope is equal to $k_q\tau_0$. Thus knowing the singlet state lifetimes of C_{70} and $C_{70}R$ in pure methylcyclohexane (0.65 ns and 1.1 ns respectively) it is possible to determine k_q. A similar plot of τ_0/τ versus [Q], results in a straight line superimposable to the first one,

$$\frac{\tau_0}{\tau} = 1 + k_q\tau_0[Q], \tag{4}$$

showing that the quenching is here overwhelmingly dynamic.

Fig. 5 shows a Stern–Volmer plot for the quenching of C_{70} both in terms of the changes in fluorescence intensity and singlet state lifetimes with increasing concentration of bromobenzene. The quenching rate constants, based on values obtained for changes in fluorescence intensity and singlet state lifetimes, were found to be identical and equal to 2.5×10^8 dm^3 mol^{-1} s^{-1}. Such results
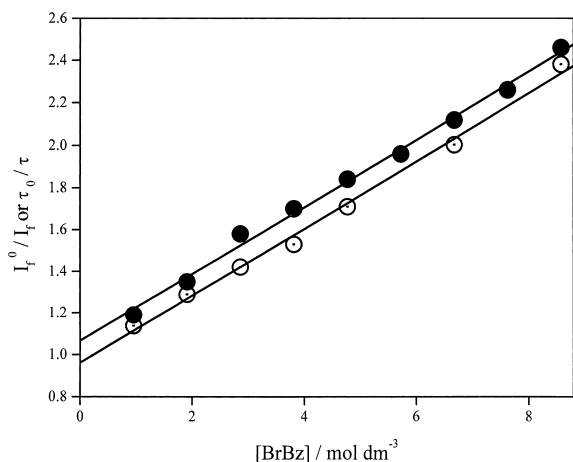
Fig. 5. Stern–Volmer plots for the quenching of C_{70} fluorescence in methylcyclohexane by bromobenzene: (⊙) lifetimes ratio (τ_0/τ) and (●) intensities ratio (I_f^0/I_f).
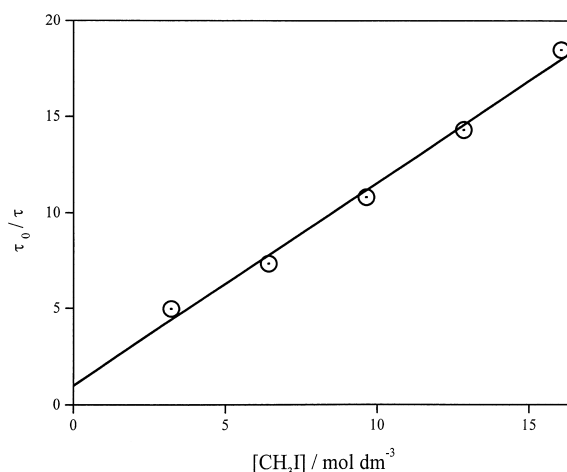

Fig. 6. Stern–Volmer plot for the quenching of $C_{70}R$ fluorescence in methylcyclohexane by CH_3I: (⊙) lifetimes ratio (τ_0/τ).

show the good agreement between the rate constants determined by the two methods.

Similar plots based on fluorescence intensity and in singlet state lifetimes (not shown) were obtained using $C_{70}R$ as the fluorophore, with a common quenching rate constant of 1.4×10^8 $dm^3\,mol^{-1}\,s^{-1}$.

To further demonstrate the order of effectiveness I > Br > Cl in terms of the ability of such substituted compounds to quench fullerene fluorescence, methyl iodide was used to quench the fluorescence of $C_{70}R$ in methylcyclohexane. A quenching rate constant of 9.6×10^8 $dm^3\,mol^{-1}\,s^{-1}$ was determined from the Stern–Volmer plot shown in Fig. 6, and is thus significantly higher than that obtained when a brominated compound was used as the quencher. All quenching rate constants observed using both changes in fluorescence quantum yields and changes in singlet state

lifetimes are collected in Tables 3 and 4 and are shown to be in good agreement with each other. It is interesting to note that even for iodinated quenchers the observed values of the quenching rate constants are still one order of magnitude lower than expected for diffusion-controlled quenching (9×10^9 $dm^3\,mol^{-1}\,s^{-1}$), this being the reason why a measurable fullerene fluorescence can still be observed in these solvents. Indeed, the Stern–Volmer straight lines obtained for mixtures of methylcyclohexane with brominated or iodinated liquid quenchers smoothly extrapolate to the solution in pure liquid quencher, cf. Figs. 5 and 6. This again indicates that the radiative rate constant is little affected by the solvent. In Tables 3 and 4 the unimolecular intersystem crossing rate constants of the perturbed fullerenes in the 1:1 complexes with the heavy atom quenchers are also given. The Stern–Volmer bimolecular rate

Table 3

Rate constants for the quenching of C_{70} fluorescence in methylcyclohexane by brominated solvents

Solvent	$k_q/10^8$ $dm^3\,mol^{-1}\,s^{-1}$ ϕ_f based	$k_q/10^8$ $dm^3\,mol^{-1}\,s^{-1}$ lifetime based	$k_{ISC}/10^9$ s^{-1}
Methylcyclohexane	0	0	1.5
Dibromomethane	2.1	1.7	1.6[a]
Bromoform	2.2	2.2	1.7[a]
Bromobenzene	2.5	2.5	1.7[a]

[a] Value for the perturbed fluorophore, computed using Eq. (6).

Table 4
Rate constants for the quenching of $C_{70}R$ fluorescence in methylcyclohexane by brominated and iodinated solvents

Solvent	$k_q/10^8 \, dm^3 \, mol^{-1} \, s^{-1} \, \phi_f$ based	$k_q/10^8 \, dm^3 \, mol^{-1} \, s^{-1}$ lifetime based	$k_{ISC}/10^9 \, s^{-1}$
Methylcyclohexane	0	0	0.91
Dibromomethane	1.1	1.0	0.99[a]
Bromoform	1.0	1.4	1.0[a]
Bromobenzene	1.4	1.4	1.0[a]
Methyl iodide	–	9.6	1.7[a]
Ethyl iodide	–	8.2	1.6[a]
Iodobenzene	–	8.3	1.5[a]

[a] Value for the perturbed fluorophore, computed using Eq. (6).

constant k_q is related to the unimolecular inter-system crossing rate constants by [22]

$$k_q = V_m \Delta k_{ISC} \qquad (5)$$

and the intersystem crossing rate constant of the perturbed fluorophore is therefore given by [22]

$$k_{ISC} = k_{ISC}^0 + \frac{k_q}{V_m} \qquad (6)$$

where

$$V_m = \frac{4}{3} \pi R^3 N_A \qquad (7)$$

and R is the collision distance for quenching (sum of the radii of the fluorophore and quencher), N_A being Avogadro's constant. For C_{70} and $C_{70}R$, a van der Waals radius of 0.53 nm was used [36]; for halogenated quenchers, the following van der Waals radii [37] were used: 0.24 nm for CH_3I, 0.25 nm for CH_2Br_2, 0.26 nm for CH_3CH_2I, 0.27 nm for $CHBr_3$, 0.29 nm for bromobenzene and 0.30 nm for iodobenzene. From the calculated values of k_{ISC}, it is seen that the effectiveness of brominated quenchers is smaller than that of iodinated ones, but that in all cases the k_{ISC} (computed for a 1:1 fluorophore–quencher complex) are not much larger than those of the unperturbed fluorophores, with a maximum increase of about 100%. However, in concentrated quencher solutions, the probability of statistical complexes with more than one heavy atom quencher is significant [22], and the average k_{ISC} is correspondingly increased. The same applies, a fortiori, to the solutions in pure liquid quenchers, cf. Tables 1 and 2, where it can

be observed that the average k_{ISC} increases by up to an order of magnitude.

3.4.3. Relevance of the quenching results for optical limiting applications

The ideal optical limiter has a normal trans-mission response below a certain incident light intensity threshold, but above that value the transmitted light intensity remains below a certain level, irrespective of the incident intensity. In fullerenes, and for not too short pulses, the optical limiting properties come from the fact that, within a broad wavelength range, triplet–triplet absorp-tion is much stronger than absorption from the singlet ground state [24–26,38]. Initial singlet–singlet absorption populates the lower triplet states by intersystem crossing. For strong nanosecond (or longer) pulses, the triplet concentration rapidly attained renders the medium much more absorb-ing well before the end of the pulse. However, for picosecond or femtosecond pulses, there is no time for triplet population build-up, since the reciprocal intersystem crossing rate constant is of the order of hundreds of picoseconds, or even a few nanosec-onds (the intrinsic fluorescence lifetime of C_{70} is ≈ 650 ps, and that of monoderivatives is of the order of one nanosecond [23]; Similar values apply to C_{60} and derivatives). Nonlinear properties are in this case due to singlet–singlet absorption from excited singlet states (mainly $S_n \leftarrow S_1$) and prob-ably also to nonsequential multiphotonic absorp-tion, but the effect is much weaker [24–26]. In this work, it was observed that in concentrated solu-tions of heavy atom quenchers, the intersystem crossing rate constant is increased by up to an

order of magnitude. This should help develop fullerenes as ultrafast responding optical limiters, on the basis of significantly reduced average time for intersystem crossing. In the case of C_{70}, the useful spectral range for this type of application lies in the near infrared, where its T–T spectrum exhibits a broad absorption band peaking at 970 nm [38]. In the case of C_{60}, whose useful spectral range covers the visible [38], preliminary results show that the enhancement of the intersystem crossing by the external heavy atom effect is comparable to that of C_{70}.

3.5. Phosphorescence

The phosphorescence spectra of both C_{70} and $C_{70}R$ have previously been reported [14,18, 24–26,31,36]. Fig. 7 shows the phosphorescence spectra for C_{70} in both MT and MTI. The phosphorescence spectrum in MT is in good agreement with previous reports, with peaks at 792, 806, 830, 846 and 884 nm. The introduction of a heavy atom in the form of iodobenzene results in approximately a fivefold increase in the intensity of the band at 806 nm, which also red shifts to 808 nm. The peak at 830 nm remains the same in intensity but blue shifts to 824 nm. Such results are in agreement with previous reports [14,18]. The overall intensity (integrated area) increases by a factor of 2.3. The increase of the phosphorescence yield is mainly due to an increased radiative con-
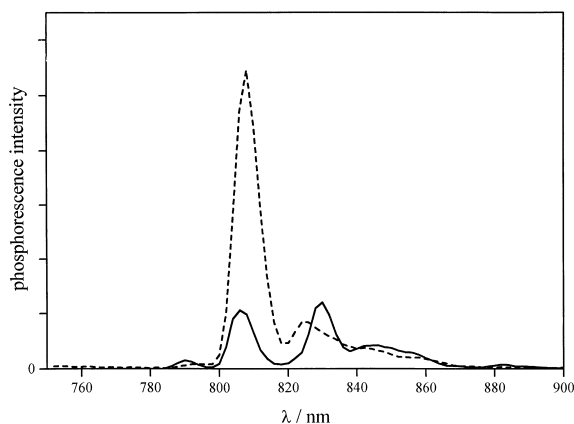
stant for phosphorescence, since the $S_1 \rightarrow T_n$ intersystem crossing has a yield already very close to one in the absence of a heavy atom effect. The measured phosphorescence lifetime at 77 K is, in MT, 42 ms, again in good agreement with previous reports [39–41]. Upon addition of iodobenzene (MTI), the phosphorescence lifetime decreases to 3.0 ms, showing that the rate constant for $T_1 \rightarrow S_0$ intersystem crossing is also increased by the heavy atom effect. The monoadduct of C_{70} shows only one emission band at 854 nm in a solution of MT, Fig. 8. The phosphorescence lifetime is 6.2 ms (Table 5). Upon addition of iodobenzene there is not only a reduction in intensity at 854 nm, but also the emergence of two new peaks at 808 nm and 830 nm. The overall intensity (integrated area) remains almost constant, increasing by a factor of 1.3. In pure iodobenzene, the 854 nm band completely disappears. In MTI the phosphorescence lifetime is 1.5 ms, half of the value for C_{70} under identical conditions. In this case, the combined
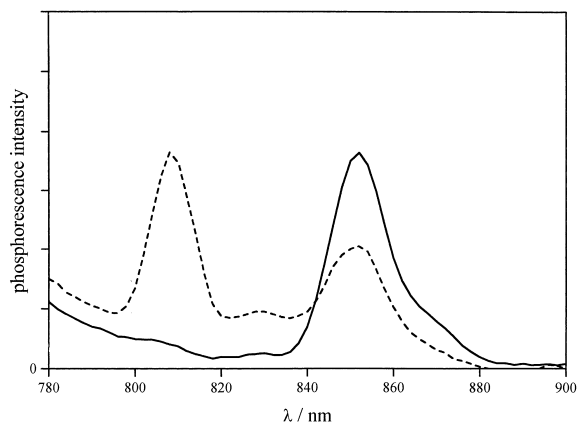

Fig. 8. Phosphorescence spectra of $C_{70}R$ in MT (—) and in MTI (- - -). Instrumental emission band pass was 9 nm.

Table 5
Phosphorescence lifetimes in ms, at 77 K

	MT[a]	MTI[b]
C_{70}	42 ± 4	3.0 ± 0.2
$C_{70}R$	6.2 ± 0.6	1.5 ± 0.1

[a] Methylcyclohexane–toluene (7:2, v/v).
[b] MT + 10% v/v iodobenzene.

Fig. 7. Phosphorescence spectra of C_{70} in MT (—) and in MTI (- - -). Instrumental emission band pass was 9 nm.

effect of $S_1 \rightarrow T_n$ enhanced intersystem crossing and increased radiative constant for phosphorescence is compensated by the increase in the rate constant for $T_1 \rightarrow S_0$ intersystem crossing owing to the heavy atom effect, and the phosphorescence quantum yield remains almost constant. The observed spectral changes in both molecules may be due to effects similar to those operating in the singlet states, but further study is required.

4. Conclusions

The fluorescence spectra, quantum yields and lifetimes of C_{70} and a pseudo-dihydro derivative ($C_{70}R$) have been measured in a wide range of solvents at room temperature. Phosphorescence spectra and phosphorescence lifetimes were also measured at low temperature. It is found that the fluorescence of C_{70} and of $C_{70}R$ are subject to quenching by halogenated compounds. Chlorinated compounds produce static quenching, attributed to weak nonfluorescent complex formation, whilst brominated and iodinated compounds originate dynamic quenching due to the external heavy atom effect. The efficiency of quenching follows the order $I > Br \gg Cl$. The external heavy atom effect is clearly displayed at 77 K in the presence of iodobenzene: $S_1 \rightarrow T_n$ and $T_1 \rightarrow S_0$ intersystem crossing processes are enhanced, the same effect being observed for the radiative constant for phosphorescence. The relative magnitude of the effects produces a slight increase of the phosphorescence quantum yield in both fullerenes, in spite of a marked phosphorescence lifetime decrease. The unimolecular intersystem crossing constant of the perturbed fluorophore in the fluorophore–quencher complex is evaluated via an original method from the bimolecular quenching constants.

In this work, it was observed that in concentrated solutions of heavy atom quenchers, the intersystem crossing rate constant is increased by up to an order of magnitude. This provides the possibility of further developing fullerenes as efficient ultrafast responding optical limiters, in cases where the triplet quantum yield is close to unity.

References

[1] F. Perrin, J. Physique 7 (1926) 390.
[2] F. Perrin, J. Chim. Physique 25 (1928) 531.
[3] F. Perrin, Fluorescence, Hermann, Paris, 1931.
[4] D.S. McClure, J. Chem. Phys. 17 (1949) 905.
[5] M. Kasha, J. Chem. Phys. 20 (1952) 71.
[6] S.P. McGlynn, R. Sunseri, N. Christodouleas, J. Chem. Phys. 37 (1962) 1818.
[7] T. Medinger, F. Wilkinson, Trans. Faraday Soc. 61 (1965) 620.
[8] S.K. Lower, M.A. El-Sayed, Chem. Rev. 66 (1966) 199.
[9] A.R. Horrocks, F. Wilkinson, Proc. Roy. Soc. Lond. A 306 (1968) 257.
[10] H. Dreeskamp, J. Pabst, Chem. Phys. Lett. 61 (1979) 262.
[11] R.S. Davidson, R. Bonneau, J. Joussot-Dubien, K.R. Trethewey, Chem. Phys. Lett. 74 (1980) 318.
[12] M.A. Morgan, G.C. Pimentel, J. Phys. Chem. 93 (1989) 3056.
[13] J.M.G. Martinho, J. Phys. Chem. 93 (1989) 6687.
[14] Y. Zeng, L. Biczok, H. Linschitz, J. Phys. Chem. 96 (1992) 5237.
[15] G. Basu, K.M. Kubasic, D. Anglos, J. Phys. Chem. 97 (1993) 3956.
[16] B.F. Minaev, S. Knuts, H. Agren, Chem. Phys. 181 (1994) 15.
[17] T.-S. Kim, Y.S. Choi, K. Yoshihara, Chem. Phys. Lett. 247 (1995) 541.
[18] S.M. Argentine, K.T. Kotz, A.H. Francis, J. Am. Chem. Soc. 117 (1995) 11762.
[19] M. Maeda, U. Graf, S. Hirayama, Chem. Phys. Lett. 257 (1996) 175.
[20] N.J. Turro, Modern Molecular Photochemistry, Benjamin, Menlo Park, CA, 1978.
[21] J.B. Birks, Photophysics of Aromatic Molecules, Wiley, New York, 1970.
[22] M.N. Berberan-Santos, Phys. Chem. Commun. (2000) 5.
[23] S. Foley, M.N. Berberan-Santos, A. Fedorov, D.J. McGarvey, C. Santos, B. Gigante, J. Phys. Chem. A 103 (1999) 8173.
[24] F. Henari, J. Callaghan, H. Stiel, W. Blau, D.J. Cardin, Chem. Phys. Lett. 199 (1992) 144.
[25] T.-H. Wei, T.-H. Huang, T.-T. Wu, P.-C. Tsai, M.-S. Lin, Chem. Phys. Lett. 318 (2000) 53.

[26] M. Konstantaki, E. Koudoumas, S. Couris, J.M. Janot, H. Eddaoudi, A. Deratani, P. Seta, S. Leach, Chem. Phys. Lett. 318 (2000) 488 and references therein.

[27] B. Gigante, C. Santos, T. Fonseca, M.J.M. Curto, H. Luftmann, K. Bergander, M.N. Berberan-Santos, Tetrahedron 55 (1999) 6175.

[28] B. Ma, Y.-P. Sun, J. Chem. Soc. Perkin Trans. 2 (1996) 2157.

[29] A. Fedorov, M.N. Berberan-Santos, J.P. Lefèvre, B. Valeur, Chem. Phys. Lett. 267 (1997) 467.

[30] Y.-P. Sun, B. Ma, C.E. Bunker, J. Chem. Soc. Chem. Commun. (1994) 2099.

[31] S.M. Argentine, A.H. Francis, C.-C. Chen, C.M. Lieber, J.S. Siegel, J. Phys. Chem. 98 (1994) 7350.

[32] A. Sassara, G. Zerza, M. Chergui, J. Phys. Chem. A 102 (1998) 3072.

[33] F. Negri, G. Orlandi, J. Chem. Phys. 108 (1998) 9675.

[34] X.L.R. Dauw, M.V. Bronsveld, A. Krüger, J.B.M. Warntjes, M.R. Witjes, E.J.J. Groenen, J. Chem. Phys. 109 (1998) 9332.

[35] R. Foster, Organic Charge-transfer Complexes, Academic Press, London, 1969.

[36] M.S. Dresselhaus, G. Dresselhaus, P.C. Eklund, Science of Fullerenes and Carbon Nanotubes, Academic Press, New York, 1996.

[37] J.T. Edward, J. Chem. Educ. 47 (1970) 261.

[38] R.V. Bensasson, T. Hill, C. Lambert, E.J. Land, S. Leach, T.G. Truscott, Chem. Phys. Lett. 206 (1993) 197.

[39] M.N. Berberan-Santos, J.M.M. Garcia, J. Am. Chem. Soc. 118 (1996) 9391.

[40] M.R. Wasielewski, M.P. O'Neil, K.R. Lykke, M.J. Pellin, D.M. Gruen, J. Am. Chem. Soc. 113 (1991) 2774.

[41] S.P. Sibley, S.M. Argentine, A.H. Francis, Chem. Phys. Lett. 188 (1992) 187.